

# Plasmadynamic synthesis of Ti-B nanopowders

**D Nikitin, A Sivkov, D Gerasimov and A Evdokimov**

National Research Tomsk Polytechnic University, 634050, Tomsk, Lenin Avenue, 30

E-mail: NikitinDmSr@yandex.ru

**Abstract.** Ti-B nanopowders were produced by plasmadynamic synthesis. This method was implemented by the synthesis in an electrodischarge plasma jet generated by a high-current pulsed coaxial magnetoplasma accelerator. Two experiments were carried out using copper and titanium conductors for initiating the plasma jet. The synthesized products were analyzed by several modern techniques including X-ray diffractometry and transmission electron microscopy. The variety of crystalline phases in the products of both Ti-B and Ti-O systems were identified. The most successful results were obtained using titanium conductors. In this case, the product mainly contains titanium boride and titanium diboride. Synthesized powder consists of hexagonal and cubic particles, which were identified as titanium boride and titanium diboride particles, respectively. The method using titanium conductors for initiating the plasma jet is more efficient and simple way for obtaining TiB/TiB<sub>2</sub> nanopowders.

## 1. Introduction

Nowadays, there is a high demand for materials with high physical and mechanical characteristics. These materials are urgently needed in the industry, particularly in the aerospace field, in the field of heavy engineering, medicine. The use of these materials helps to reduce maintenance and repair costs of technical equipment, increases their service life, allows obtaining easier and cheaper construction, as well as reducing the risk of accidents.

Titanium diboride has high hardness and has high abrasive properties and resistivity to metal melts [1]. It is a refractory material, so it is increasingly used in industry at high temperatures and in aggressive environments [2]. Titanium diboride TiB<sub>2</sub> does not react with molten steel, cast iron, Zn, Cd, Sn, Pb, Bi, weakly reacts with copper at temperatures above 1400 °C [3]. This makes it possible to produce thermocouples and their protective covers, as well as a variety of lining materials and details for metallurgical furnaces. Titanium diboride is used for production of evaporators for molten metals and electrolytic cells lining, as a component of high-temperature alloys, tool materials, wear-resistant surfacing coatings [4]. Borides of titanium are required in the manufacture of jet engine parts, gas turbine blades [5]. The high hardness allows using borides as abrasives providing a higher surface when processing ductile metals and alloys than synthetic diamond grinding [6].

Titanium diboride and boride particles with micro- and nanometer dimensions are known to improve the strength and creep resistance of metal-matrix composites [7]. Nanoceramics based on titanium borides has greater fracture toughness, ductility and ease of densification compared with conventional titanium borides ceramics [7]. Therefore, one of the ways to improve ceramics properties is creation of nanoceramics. The most common methods of TiB<sub>2</sub>/TiB nanopowder synthesis are mechanochemical synthesis, self-propagating high-temperature synthesis, sol-gel reduction [8].



The present paper reports a novel method of direct and quick production of nanodispersed Ti-B phases by a plasmadynamic technique. This method has been already successfully used for synthesis of different nanopowders and nanocoatings (including nano-SiC, TiN, WC and etc.) [9], [10].

## 2. Experimental Conditions

The paper presents the results of experimental and analytical studies on the synthesis of nanocrystalline powders containing in its composition phase diboride and titanium boride. Required conditions for obtaining a compound of titanium and boron are provided in high energy impact of a high-speed (about  $10^3$  m/s), high-density ( $>1.0$  g/cm<sup>3</sup>) and high-temperature ( $\sim 1000$  K) discharge plasma jet. Such a plasma jet was generated by a coaxial magnetoplasma accelerator of a high current ( $\sim 10^5$  A) discharge of Z-pinch type. The process of generating a plasma jet, implementation of the chemical reactions and formation of the final product takes a short time ( $\sim 1.0$  ms). The generated plasma jet was accelerated by the magnetic field of an accelerating channel and an inductor (a solenoid).

The main metal component for the synthesis of metal compounds was introduced into the system by means of electroerosion of titanium from surface of a titanium accelerating channel of magnetoplasma accelerator. The second main component (amorphous boron) in form of powder was placed into the plasma formation zone. Due to the use of a dielectric precursor in the plasma formation zone there was a problem of initiating the plasma bridge between the central electrode and the accelerating channel. Figure 1 shows the unit of a central electrode with applied method initiating a plasma jet. Amorphous boron powder was placed axially into plasma formation zone (4) as a precursor of a chemical reaction. Thin metal conductors (3) were stretched between central electrode (1) and coaxial electrode (2) along the surface of the plasma formation zone in order to initiate arc discharge in dielectric space. Two experiments were carried out using copper (1) and titanium (2) conductors for initiating the plasma jet. Plasma shots were produced in a sealed volume of the cylindrical reactor chamber filled with argon at normal pressure and room temperature.

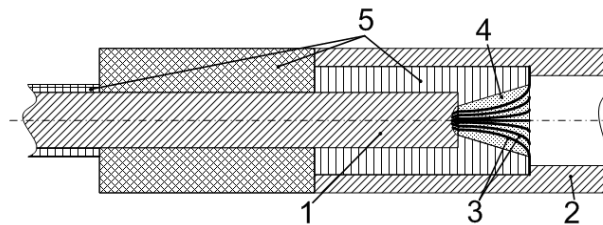


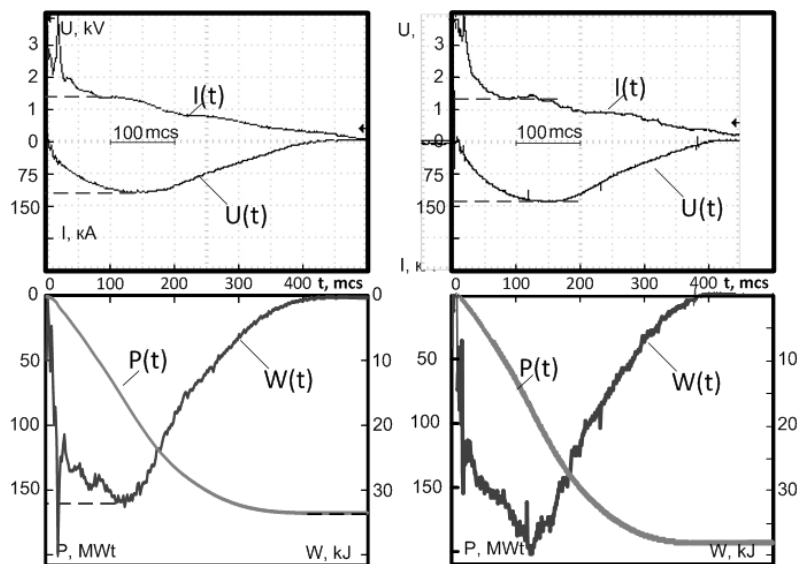
**Figure 1.** The unit of a central electrode of a coaxial magnetoplasma accelerator: central electrode (1), coaxial electrode (2), copper/titanium conductors (3), plasma formation zone (4), insulators (5).

A magnetoplasma accelerator was supplied by a capacitive energy storage with the maximum stored energy  $W_{\max} = 360$  kJ. The electrical and energy parameters of the experiments are presented in Table 1. Figure 2 shows the oscillograms of operating current  $I$ , the voltage on the electrodes of magnetoplasma accelerator  $U$ , the discharge power  $P$ , the released energy  $W$  obtained by a Tektronix TDS1012 oscilloscope. According to these waveforms and tables, explosive material of conductors does not practically affect the energy release in the process. Opening a chamber reactor and collecting the powdered product was performed with almost complete deposition of suspended particles on the walls of a chamber. This time is the time of passivation powder in argon atmosphere.

Synthesized in the experiments powder products were analyzed without any preparation by such modern methods as X-ray diffraction (XRD) using Shimadzu XRD 6000 diffractometer (Cu  $K\alpha$ -radiation,  $\lambda = 0.15406$  nm), transmission electron microscopy (TEM) using Philips CM 12 microscope. Qualitative X-ray analysis was made by PowderCell 2.4 software package using PDF4+ database.

**Table 1.** Electrical and energy parameters of the experiments.

Exp.	Method of initiating	$m_{\text{pow}}$ [g]	$I_{\text{max}}$ [A]	$U_w$ [kV]	$P_{\text{max}}$ [MW]	$W_c$ [kJ]	$W$ [kJ]
1	Cu-cond.	3.5	120	1.40	155	67.5	33.5
2	Ti-cond.	3.2	140	1.40	201	67.5	38.3

**Figure 2.** Oscillograms of operating current  $I$ , the voltage on the electrodes of magnetoplasma accelerator  $U$ , the discharge power  $P$ , the released energy  $W$ .

### 3. Results and discussion

The XRD patterns of the products obtained with the use of copper and titanium conductors are shown in Figure 3. The identified peaks are marked in the diffraction patterns. The analysis showed that the synthesis product of experiment 1 (the use of Cu-conductors as a method of initiating) contains crystalline phases:  $\text{TiB}_2$  (ICDD Card No. 00-07-0275; hexagonal, space group  $P6/mmm$ , No. 191),  $\text{TiB}$  (ICDD Card No. 00-06-0641; cubic, space group  $Fm\bar{3}m$ , No. 225),  $\text{Ti}$  (ICDD Card No. 00-01-1197; hexagonal, space group  $P63/mmc$ , No. 194),  $\text{TiO}_2$  (ICDD Card No. 00-49-1433; orthorhombic, space group  $Pbnm$ , No. 62),  $\text{TiO}_2$  (ICDD Card No. 00-76-0326; tetragonal, space group  $P42/mnm$ , No. 136),  $\text{TiO}_2$  (ICDD Card No. 00-82-0514; tetragonal, space group  $P42/mmm$ , No. 136),  $\text{TiB}$  (ICDD Card No. 00-05-0700; orthorhombic, space group  $Pnma$ , No. 62). Quantitative XRD analysis was performed only for the synthesis product of the experiment 2 (the use of Ti-conductors as a method of initiating) due to the multicomponent product of the powder synthesized in experiment 1. Quantitative XRD analysis is presented in Table 1.

The variety of crystalline phases in the products of both Ti-B and Ti-O systems were identified. The presence of oxygen in the products in the forms of several titanium oxides  $\text{TiO}_2$  (including different crystal systems) were caused by usage of commercially pure boron, which included a small quantity of boron oxide. As a result of the transition of oxygen into the plasma state, titanium—which is more reactive than boron—entered into chemical reactions of compound with oxygen, and the formation of several oxides occurred. The products also contain boride of titanium and diboride of titanium. The preferential content of borides in the products compared with diboride is explained by the certain ratio of boron and titanium for respective phases in accordance with the Ti-B state diagram [11], 20% of boron in the system. The products contain pure titanium, and this fact demonstrates the excess of titanium in the system. Also, the diffraction patterns contain the amorphous halo at low angles characteristic for a product including an amorphous phase. In these cases, such an amorphous phase is pure boron, which was placed into the plasma formation zone. The boron had not been able to

react with titanium because of the sharp process of electrical explosion of conductors, and it was rapidly taken out of the chemical reaction zone to the reactor chamber in the unreacted state by a hypersonic plasma jet. It should be noted that the diffraction pattern of experiment 1 has a halo at low angles with larger area indicating a greater weight of amorphous boron in the product. It corresponds to a sharper process of electrical explosion reflected by the oscillograms (Figure 2).

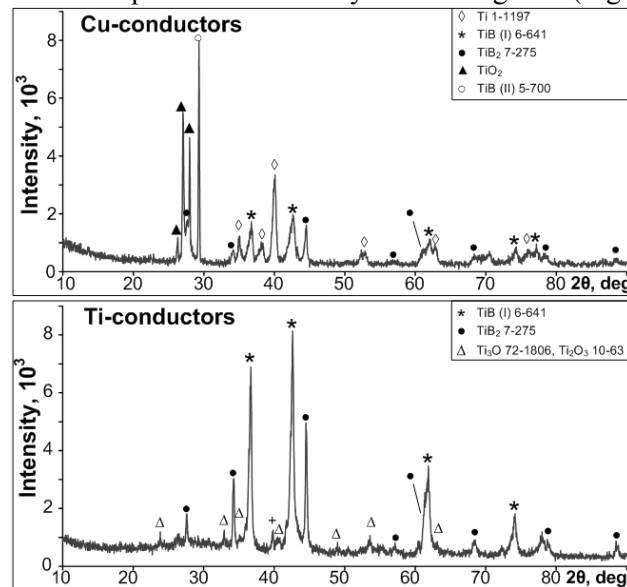


**Figure 3.** Diffraction patterns of the synthesized powders.

**Table 2. Quantitative XRD analysis.**

	Contents of phases ( $\omega$ ); CSR			$R_{wp}/R_{exp}$
	TiB <sub>2</sub>	TiB/TiN	Ti-hex	
$\omega$ [%]	24.50	69.50	6.00	25.8/9.8
CSR [nm]	90.3	47.4	32.5	

A smaller amount of crystalline phase in the product was identified in the experiment 2, as it can be seen from the corresponding diffraction pattern (Fig. 3) and the results of the quantitative XRD analysis (Table 1). The main synthesized phases are hexagonal titanium diboride TiB<sub>2</sub> and cubic titanium boride TiB. The values of goodness S ( $R_{wp}/R_{exp}$ ), which take values >1, indicate the correctness of calculations. The calculation revealed a high content of titanium boride corresponding to a state diagram at low content of titanium and low temperatures of formation. According to the values of coherent scattering areas (CSA) in Table 2, all the phases are nanodispersed.

The product of experiment 2 was analyzed by transmission electron microscopy (Figure 4). According to the obtained images, the synthesized powder includes crystalline agglomerates of particles with sizes up to several hundred nanometers. Figure 4a shows the bright field image. There are several types of particles in the powdered product. The first type (1) is particles of a round or hexagon shape. The first type can be referred to a space group P6/mmm of titanium diboride. The second type (2) is particles of square shape. The second type can be referred to a space group Fm3m of titanium boride. The selected area electron diffractions (SAED) are presented in Figures 4b and 4d. The most striking and the main diffraction reflexes relate to reflecting planes of titanium diboride and titanium boride. The dark-field images (Figures 4c and 4e) prove accordance of the mentioned types of particle with titanium diboride boride and titanium boride.

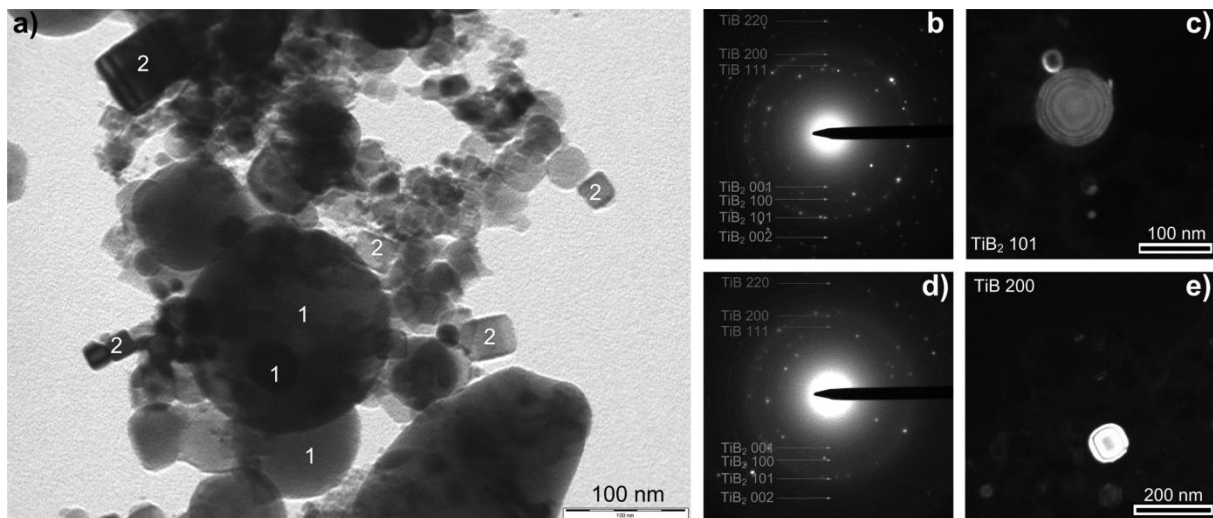


**Figure 4.** TEM-images of the plasmadynamic synthesis product: (a) bright field image, (b), (d) SAED, (c), (e) dark-field images.

#### 4. Conclusions

Ti-B nanopowders were produced by plasmadynamic synthesis. This method was realized by the synthesis in electrodischarge plasma jet generated by a high-current pulsed coaxial magnetoplasma accelerator. Two experiments were carried out using copper and titanium conductors for initiating the plasma jet. The synthesized products were analyzed by several modern techniques including X-ray diffractometry and transmission electron microscopy. The variety of crystalline phases in the products of both the system Ti-B and Ti-O were identified. The most successful result was obtained using titanium conductors. In this case, the product mainly contains titanium boride and titanium diboride. The synthesized powder consists of hexagonal and cubic particles, which were identified as titanium boride and the titanium diboride particles, respectively. The method using titanium conductors for initiating the plasma jet is a more efficient and simple way for obtaining TiB/TiB<sub>2</sub> nanopowders.

#### References

- [1] Basu B, Raju G B, Suri A K 2006 *Int. Mater. Rev.* **51** 352
- [2] Carenco S, Portehault D, Boissiere C, Mezailles N, Sanchez C 2013 *Chem. Rev.* **113** 7981
- [3] Andrievski R A 2015 *Russ. Chem. Rev.* **84** 540
- [4] Ravi Chandran K S, Panda K B, Sahay S S 2004 *JOM* **56** 42
- [5] Saito T 2004 *JOM* **56** 33
- [6] Munro R G. 2000 *J. Res. Natl. Inst. Stand. Technol.* **105** 709
- [7] Bates S E, Buhro W E, Frey C A, et al. 1995 *J. Mater. Res.* **10** 2599
- [8] Nozari A, Heshmati-Manesh S, Ataie A 2012 *Int. J. Refract. Met. Hard Mater.* **33** 107
- [9] Sivkov A, Nikitin D, Pak A, Rakhmatullin I 2015 *Nanotechnologies Russ.* **10** 34
- [10] Pak A, Sivkov A, Shanenkov I, Rahmatullin I, Shatrova K 2015 *Int. J. Refract. Met. Hard Mater.* **48** 51
- [11] Murray J L, Liao P K, Spear K E 1986 *Bull. Alloy Phase Diagrams.* **7** 550

#### Acknowledgments

This work was supported by the Russian Science Foundation (project no. 15-19-00049).